Bio-inspired Scaly Cu/Ag Coating on Regenerated Cellulose Fiber *via* Self-Assembly for Facile Motion Sensing

Qing Wang [a,b,c] Hong Zhao,[c] Heng Zhao,[c] Yongmei Zeng,[a] Jinguang Hu,[c] and Fei Shen, [a]*

* *Corresponding author: fishen@sicau.edu.cn*

DOI: 10.15376/biores.21.2.4607-4619

GRAPHICAL ABSTRACT

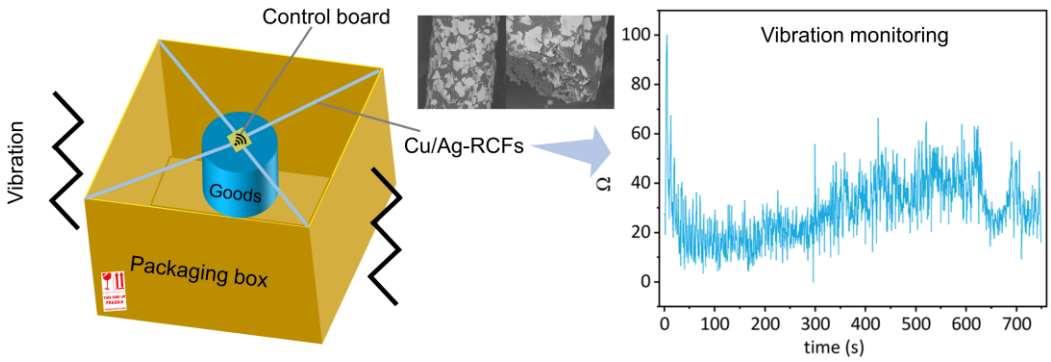

Bio-inspired Scaly Cu/Ag Coating on Regenerated Cellulose Fiber *via* Self-Assembly for Facile Motion Sensing

Qing Wang [a,b,c] Hong Zhao,[c] Heng Zhao,[c] Yongmei Zeng,[a] Jinguang Hu,[c] and Fei Shen, [a,*]

A facile, scalable, and bioinspired approach was used to create a high-performance, biodegradable motion sensing through the construction of a scaly conductive coating on regenerated cellulose fibers (RCFs) derived from bacterial cellulose. A single-step dip-coating process enabled the *in situ* self-assembly of copper nanoplates and silver nanoparticles into a multilayered, overlapping architecture during controlled fiber withdrawal, mimicking the flexible yet robust structure of fish scales. The obtained Cu/Ag-RCFs sensor exhibited an exceptional balance of mechanical durability, electrical conductivity, and tunable electromechanical response. Their sensitivity and dynamic range could be precisely tailored by adjusting the number of coating cycles, with the optimized device (4 cycles) delivering stable, reversible, and highly reproducible resistance changes under both bending and tensile deformations. Practical applicability was demonstrated through preliminary demonstrations, including successful integration into a glove for real-time finger gesture recognition and deployment as a vibration monitor for intelligent logistics. Critically, the cellulose-based substrate ensured environmental sustainability, maintaining operational stability in aqueous environments while enabling rapid, complete degradation in acidic or enzymatic conditions. This work establishes a novel paradigm for sustainable electronics that harmonizes bioinspired design, high sensing performance, and end-of-life biodegradability.

DOI: 10.15376/biores.21.2.4607-4619

Keywords: Regenerated cellulose fiber; Dip-coating; Self-assembly; Bio-inspired sensor; Motion detection; Wearable device

*Contact information: a: College of Environmental Sciences, Sichuan Agricultural University, Chengdu, Sichuan 611130, P. R. China; b: Chengdu Academy of Agriculture and Forestry Sciences, Chengdu, Sichuan 611130, P. R. China; c: Chemical and Petroleum Engineering, Schulich School of Engineering, University of Calgary, Calgary T2N 4H9, Canada; *Corresponding author: fishen@sicau.edu.cn*

INTRODUCTION

Flexible and wearable electronics have garnered significant attention in recent years due to their potential applications in human motion monitoring, health diagnostics, soft robotics, and smart textiles (Gao *et al.* 2019; Peng *et al.* 2021). Among the various sensing mechanisms, resistive-type strain sensors based on conductive fibers stand out for their simple structure, low power consumption, and compatibility with textile integration (Huang *et al.* 2022). However, achieving high sensitivity, wide sensing range, mechanical durability, and environmental sustainability simultaneously remains a challenge (Luo *et al.* 2023).

Natural biopolymers offer a promising alternative to conventional petroleum-based substrates, owing to their renewability, biodegradability, and excellent mechanical properties. Cellulose, the most abundant natural polymer on Earth, has emerged as a particularly attractive candidate for flexible electronics (Ummartyotin and Manuspiya 2015; Rajendran *et al.* 2025). When processed into regenerated cellulose fibers (RCFs), it exhibits high tensile strength, good flexibility, biocompatibility, biodegradability, and abundant surface hydroxyl groups that facilitate chemical or physical functionalization (Shen *et al.* 2023; Wang *et al.* 2023). These properties make RCFs an ideal green platform for building electronic devices. RCFs can be produced through various routes, including the traditional viscose process, dissolution in ionic liquids or *N*-methylmorpholine-*N*-oxide (NMMO), *N*, *N*-Dimethylacetamide (DMAc)/LiCl, and direct wet-spinning from bacterial cellulose pellicles (Huber *et al.* 2025). Nevertheless, the intrinsic electrical insulation of cellulose necessitates the integration of conductive materials to create functional sensors, a process that must be efficient, economical, and should ideally preserve or enhance the material's desirable mechanical properties (Zhao *et al.* 2021). To endow RCFs with electrical conductivity, a variety of strategies have been explored, including *in-situ* polymerization of conductive polymers (*e.g.*, polyaniline), deposition of carbon nanomaterials (*e.g.*, graphene, carbon nanotubes), and metallization via sputtering or electroless plating (Saleh *et al.* 2025). While effective, many of these approaches suffer from complex processing, poor scalability, or the use of toxic reagents. In contrast, dip-coating with commercial conductive paints offers a facile, low-cost, and scalable route suitable for industrial adoption (Wang *et al.* 2023; Okokpujie *et al.* 2024).

Drawing inspiration by nature's elegant solutions to complex engineering challenges, this study takes cues from the structure of fish scales (Fig. 1). The overlapping and sliding arrangement of scales enables fish to simultaneously achieve flexibility and mechanical protection, a principle highly relevant to flexible sensor that must sustain electrical conductivity under deformation. By emulating this bio-inspired "scaly" architecture, the authors propose a promising strategy for constructing conductive networks capable of maintaining robust electrical pathways during bending or stretching.

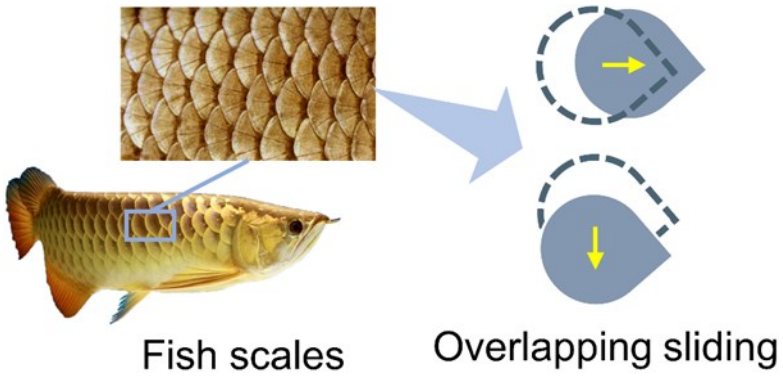

Fig. 1. Bio-inspired design principle: Schematic illustration of the overlapping and sliding arrangement of fish scales during body bending, which serves as the structural model for the conductive coating on RCFs

This article reports a facile and scalable strategy for fabricating a high-performance, biodegradable motion sensor by constructing such a bio-inspired scaly Cu/Ag coating on RCFs *via* a multi-cycle dip-coating and drying process. The resulting Cu/Ag-RCFs exhibited excellent conductivity, a wide sensing range, and high gauge factor, enabling

real-time detection of subtle human motions and environmental vibrations. Practical applicability was confirmed through preliminary demonstrations, including successful integration into a glove for gesture recognition and deployment as a vibration monitor for goods transportation. This work provides a preliminary yet novel paradigm for fabricating high-performance cellulose-based sensors that balance functionality, sustainability, and manufacturability.

EXPERIMENTAL

Materials and Wet-spinning of RCFs

Bacterial cellulose (BC) was used as the precursor for the preparation of regenerated cellulose fibers (RCFs). The BC was obtained from a previous study in which *Acetobacter xylinum* ATCC 23767 was cultured on sweet sorghum as the carbon source (Wang *et al.* 2021). Prior to processing, the BC pellicles were ground using an IKA A11 basic analytical mill (IKA-Werke, Germany) and subsequently passed through a 40-mesh sieve. The resulting powder was then vacuum-dried at 60 °C for 24 h to remove residual moisture. *N,N*-Dimethylacetamide (DMAc, Sigma-Aldrich, Cat. No. D137510-2.5L) and lithium chloride (LiCl, Sigma-Aldrich, Cat. No. 793620-500G) were used as received, except that LiCl was pre-dried under vacuum at 150 °C for 6 h to ensure anhydrous conditions. To enhance solubility, 1.00 g of dried BC was dispersed in 50 mL of DMAc and stirred at 100 °C for 60 min. The solvent was subsequently removed by vacuum drying at 60 °C for 48 h, yielding activated BC. This material was then dissolved in a pre-saturated DMAc/LiCl solution by heating at 100 °C for 60 min, followed by continuous stirring at room temperature until a homogeneous, viscous cellulose solution was obtained (Wang *et al.* 2023). The resulting dope was loaded into a sealed syringe and degassed by centrifugation at 3000 rpm for 5 min to eliminate entrapped air bubbles. The solution was then extruded through a stainless-steel spinneret into an ethanol coagulation bath using a GC pump (flow rate: 2.0 mL/min) to regenerate the RCFs. The freshly spun RCFs were continuously collected onto a rotating drum and air-dried at ambient conditions.

Preparation of Cu/Ag-RCFs

A commercial water-based copper/silver conductive paint (Super Shield™ 843WB), that was kindly supplied by M.G. Chemicals (Burlington, Canada) was chosen to fabricate the conductive coating. This formulation contains approximately 22 wt.% copper nanoplates, 4 wt.% silver nanoparticles, and an aqueous polymer binder.

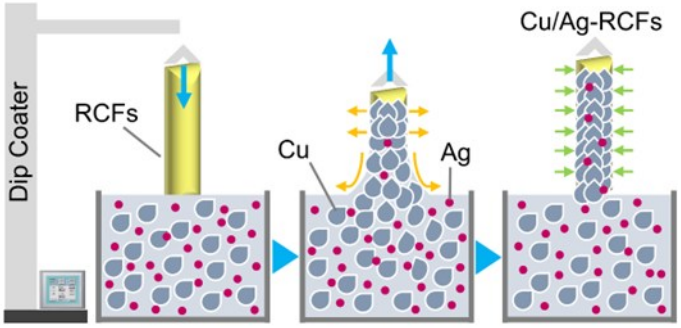

Fig. 2. Schematic illustration of the dip-coating process for the self-assembly of the bio-inspired scaly Cu/Ag conductive coating on the RCFs

As illustrated in Fig. 2, the RCFs substrate was mounted on a PTL-MM02-200 dip coater (MTI, Canada) and vertically immersed into the conductive paint for 5 s. The fiber was then withdrawn at a constant speed of 10 mm/min, during which the copper flakes self-assembled into a scale-like morphology, completing one coating cycle. The coated fiber (denoted as Cu/Ag-RCFs) was then allowed to dry at room temperature for 20 min to allow partial solvent evaporation and structural stabilization. This dip-coating and drying cycle was repeated 2 to 5 times to construct a multi-layered conductive structure. Following the final cycle, the resulting Cu/Ag-RCFs was dried at room temperature for 24 h to ensure complete solidification and optimal performance of the conductive layer.

Characterizations

The morphology and elemental composition of the samples were examined using a Phenom Pro-X scanning electron microscope equipped with energy-dispersive X-ray spectroscopy (SEM/EDS, Phenom, Netherlands). Imaging was carried out at an accelerating voltage of 15 kV, and elemental mapping was acquired at a resolution of 128 × 128 pixels.

Tensile properties of both RCFs and Cu/Ag-RCFs were evaluated using an MT-1528 universal tensile tester (Qualitest, USA) equipped with a 100 N load cell. Tests were conducted at a constant crosshead speed of 10 mm/min with an initial gauge length of 20 mm. Five replicates were tested for each sample to ensure statistical reliability.

The strain- and bending-dependent sensing performance of Cu/Ag-RCFs was characterized using a custom-built setup integrating the tensile tester, a Keithley 2000 (Keithley, USA) digital multimeter, and a computer for synchronized data acquisition. The sensor was mounted between custom-modified clamps, and its two terminals were connected directly to the multimeter *via* copper wires using a standard two-electrode configuration. Resistance measurements were performed in two-wire ohmmeter mode with auto-ranging enabled. During testing, mechanical displacement (or bending angle) was precisely controlled by the tensile tester under computer command, while the electrical resistance was simultaneously recorded at 50/s sampling rate.

The relative resistance change, $\Delta R/R_0$, was calculated according to Eq. 1,

$$\Delta R/R_0 = (R_1 - R_0)/R_0 \quad (1)$$

where R_0 is the initial resistance at the undeformed state, and R_1 is the instantaneous resistance during deformation. Sensor sensitivity (S) was defined as Eq. 2,

$$S = (\Delta R/R_0)/\Delta M \quad (2)$$

where ΔM represents the actuation parameter, either tensile strain (expressed as % elongation) or bending angle (in degrees), depending on the test mode.

Controlled degradation tests were carried out by immersing the sensors in three different media: deionized water (as control), 72 wt% sulfuric acid solution, and a cellulase solution (40 FPU/g). A parallel control test was carried out in deionized water for comparison. All experiments were conducted at room temperature under static conditions, and morphological changes were monitored over time to assess biodegradability.

Statistical Analysis

All raw data were exported from the native software of the respective instruments and processed using OriginPro 2024 (OriginLab Corp., USA) for statistical analysis, curve fitting, and graphical visualization.

RESULTS AND DISCUSSION

Morphological and Structural Characterization

The successful fabrication of regenerated cellulose fibers (RCFs) and their subsequent functionalization with a conductive coating were first verified through morphological and elemental analyses. As shown in Fig. 3a, the original RCFs exhibited a smooth and uniform surface morphology, consistent with that of wet-spun cellulose fibers reported previously (Wang *et al.* 2023). After dip-coating process, a pronounced change in the surface topography was observed. The Cu/Ag-RCFs (Fig. 3b, c) displays a continuous, hierarchical conductive layer featuring an overlapping, scale-like architecture reminiscent of natural fish scales.

This bio-inspired scaly morphology was further confirmed by cross-sectional SEM imaging (Fig. 3d), which revealed a well-defined multi-layered coating firmly adhered to the RCF substrate. A high-magnification inset clearly shows that the conductive layer consisted of densely packed copper flakes embedded in a polymeric binder matrix (the silver nanoparticles are not directly visible here due to their small size). The formation of this scale-like network provides direct visual evidence of the self-assembly process driven by controlled withdrawal during dip-coating. Energy-dispersive X-ray spectroscopy (EDS) further corroborated the composition and homogeneity of the coating. The EDS spectrum (Fig. 3e) and corresponding elemental maps (Fig. 3f-h) confirm the uniform distribution of Cu and Ag elements across the fiber surface, while the C signal originated from both the underlying cellulose substrate and the aqueous polymer binder. This homogeneous dispersion of conductive fillers is essential for establishing percolated electrical pathways and ensuring reliable, reproducible sensing performance.

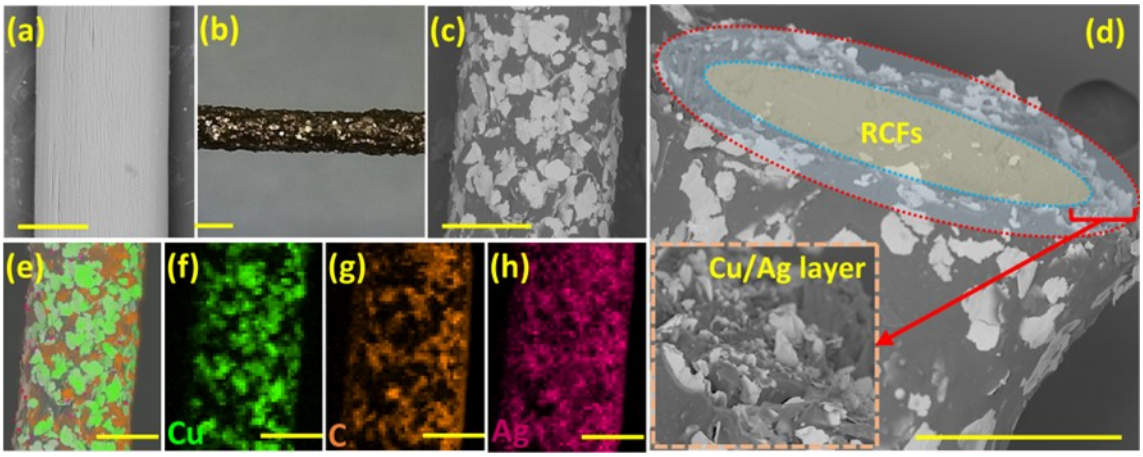

Fig. 3. Morphological and elemental characterization of RCFs and Cu/Ag-RCFs. (a) SEM image of original RCFs; (b) Optical photograph of Cu/Ag-RCFs; (c) surface SEM image of Cu/Ag-RCFs; (d) Cross-sectional SEM image of Cu/Ag-RCFs; (e) EDS spectrum of the Cu/Ag-RCFs surface; Elemental mapping of copper (f), carbon (g), and silver (h); Scale bars: 200 μm

Mechanical, Electrical, and Sensing Properties of Cu/Ag-RCFs

The integration of a rigid metallic coating onto a flexible cellulose substrate introduces a complex trade-off among mechanical integrity, electrical conductivity, and sensing functionality (Chen *et al.* 2021). As shown in Fig. 4a, original RCFs exhibited excellent tensile properties typical of wet-spun cellulose fibers, with a high tensile strength of 529 MPa and a Young's modulus of 8.10 GPa. After dip-coating (3 cycles), the Cu/Ag-

RCFs displayed reduced tensile strength (302 MPa) and modulus (4.96 GPa), accompanied by a significant increase in fracture strain from 23% to 40% and retained high toughness (98 MJ/m³).

This mechanical transition is attributed to partial plasticization of the cellulose matrix during the aqueous dip-coating process (Zhao *et al.* 2021). Water molecules disrupt the intermolecular hydrogen-bonding network within the RCFs, thereby reducing stiffness while enhancing ductility, a phenomenon consistent with prior observations (Wang *et al.* 2023).

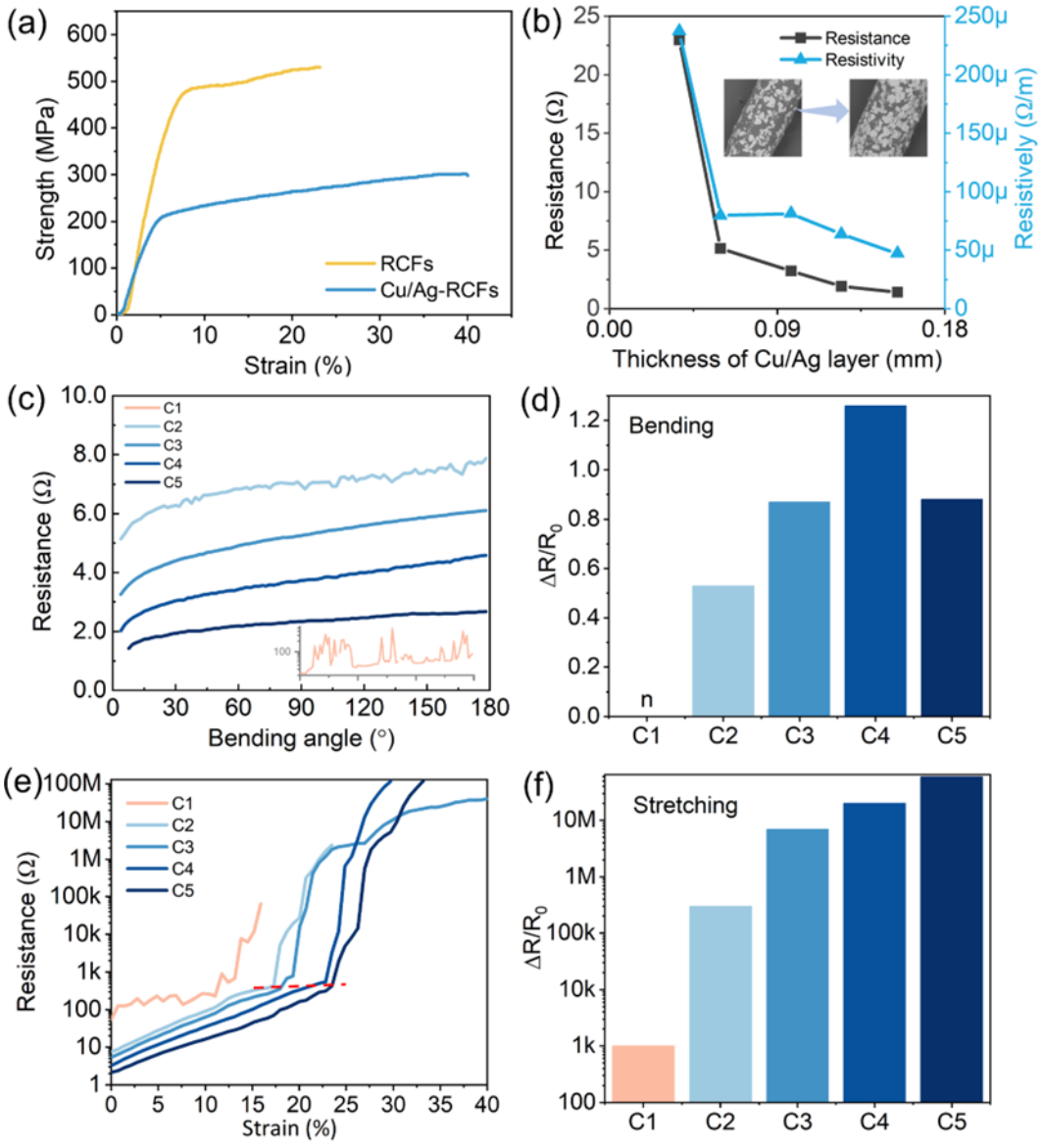

Fig. 4. Mechanical, electrical, and electromechanical sensing properties of RCFs and Cu/Ag-RCFs. (a) Tensile stress-strain curves. (b) Coating thickness, electrical resistance, and resistivity of Cu/Ag-RCFs as a function of the number of coating cycles. (c) Real-time resistance response and (d) corresponding relative resistance change ($\Delta R/R_0$) of Cu/Ag-RCFs during bending deformation for sensors with 1–5 coating cycles. (e) Real-time resistance response and (f) corresponding relative resistance change ($\Delta R/R_0$) of Cu/Ag-RCFs with 1–5 coating cycles under tensile strain

The tight interface between the coating and fiber core observed in the cross-sectional SEM image (Fig. 3d) further supports solvent penetration and interfacial interaction. Crucially, the scaly, overlapping architecture of the conductive layer does not induce catastrophic brittleness; instead, it accommodates large deformations through sliding between adjacent metallic flakes, preserving the flexibility required for wearable applications.

The dip-coating process effectively converted the insulating RCFs into highly conductive fibers. Figure 4b summarizes the evolution of coating thickness, electrical resistance, and resistivity as a function of deposition cycle number. With increasing the cycles from 1 to 5, the coating thickness rose from 37.5 to 154.5 μm, while the two-terminal resistance dropped dramatically from 23 to 1.42 Ω. More significantly, the calculated resistivity decreased from 2.37×10^{-4} to 4.71×10^{-5} Ω·m, indicating the formation of a more dense, continuous, and percolated conductive network with each subsequent layer. This layer-by-layer enhancement in electrical continuity provides the foundation for high signal-to-noise ratio (SNR) in subsequent sensing applications (Ma *et al.* 2021).

The core sensing functionality of Cu/Ag-RCFs was evaluated by monitoring the relative resistance change ($\Delta R/R_0$) in response to mechanical deformation. Under bending (Fig. 4c), a single-coating sensor exhibited erratic, non-reproducible responses with resistance fluctuations spanning orders of magnitude, indicative of an incomplete, discontinuous conductive network prone to random fracture and reconnection. In contrast, Cu/Ag-RCFs with 2 to 5 coating cycles demonstrated smooth, stable, and reversible responses. The resistance increased monotonically with bending angle due to progressive separation of the overlapping "scales", which elevates inter-flake contact resistance.

As quantified in Fig. 4d, the Cu/Ag-RCFs with 4 coating cycles achieved the highest bending sensitivity ($\Delta R/R_0 = 1.26$). This optimum is proposed to arise from a balanced microstructure: too few numbers of coatings (*e.g.*, 1 to 2 cycles) yield sparse scale coverage with poor mechanical stability and low SNR, whereas excessive coating cycles (*e.g.*, 5 cycles) form an overly thick, quasi-continuous metallic film that behaves more like a rigid conductor rather than a responsive sensing structure, thereby diminishing deformation-induced resistance modulation. Thus, the 4-cycle coating is proposed to represent a balance, where the structure is robust enough to maintain stable electrical pathways while remaining sufficiently responsive to mechanical deformation.

Under tensile strain (Fig. 4e), all Cu/Ag-RCFs exhibited two distinct regions, as clearly demarcated by the red dashed line. The region below this line (low strain) was characterized by a linear and reversible increase in resistance, which was governed by elastic sliding within the scaly network. This behavior makes the low-strain region ideal for precise and repeatable strain detection. Beyond this threshold (high strain), a sharp, non-linear, and irreversible resistance surge occurred, signaling microcrack initiation and permanent damage in the conductive layer. Notably, the upper limit of the linear regime expanded with more coating cycles; for instance, the sensor with 5 coating cycles maintained stable linearity up to higher strains compared to the one with 2 cycles, owing to its thicker, more resilient conductive scaffold. Consequently, the maximum $\Delta R/R_0$ value before failure soared from 7 k to 60 M (Fig. 4f), demonstrating an extraordinary dynamic range tunable *via* coating design.

The quantitative relationship between mechanical input and electrical output was systematically analyzed *via* curve fitting, with results summarized in Table 1. For bending deformation, the $\Delta R/R_0$ response was best described by a cubic polynomial (y = Intercept + $B_1x + B_2x^2 + B_3x^3$), reflecting the nonlinear separation dynamics of the scale-like structure.

As the number of coating layers increased from 2 to 5, both the intercept and polynomial coefficients consistently decreased, indicating that a denser conductive network required greater deformation to elicit a measurable resistance change, effectively shifting the sensor's operating window toward higher actuation levels.

In contrast, the tensile response followed a linear model (y = Intercept + Slope·x), characteristic of classical piezoresistive behavior. The slope gradually decreased from 0.1070 to 0.0922 with increasing layer number, suggesting that while thicker coatings enhance baseline conductivity (Fig. 4b), they slightly reduce strain sensitivity due to increased structural rigidity. Critically, the coefficient of determination (R^2) for both bending and stretching models approached unity (>0.99) for sensors with ≥2 cycles, confirming highly predictable and reproducible electromechanical responses, and this is an essential prerequisite for practical sensing applications.

Collectively, these results indicate that, within the scope of the Cu/Ag-RCFs system investigated here, the number of dip-coating cycles serves as a simple and effective parameter to tailor the multifunctional performance. Under the experimental conditions employed, adjusting this variable enabled a tunable balance among electrical conductivity, mechanical compliance, sensitivity, and operational range, demonstrating the potential of this approach for applications such as joint motion tracking or large-deformation monitoring in similar fiber-based sensing platforms.

Table 1. Fitting Parameters for the Electrical Response of Cu/Ag-RCFs as a Function of Coating Cycles under Bending and Stretching Deformation

	Bending					Stretching		
Coating cycles	B1	B2	B3	Intercept	R^2	Slope	Intercept	R^2
1	-	-	-	-	-	0.0355	2.04	0.5312
2	0.0447	-3.83E-4	1.20E-6	5.27	0.9749	0.1070	0.90	0.9961
3	0.0374	-2.39E-4	6.53E-7	3.40	0.9945	0.1024	0.78	0.9969
4	0.0323	-2.28E-4	6.97E-7	2.19	0.9932	0.0973	0.57	0.9990
5	0.0174	-1.09E-4	2.82E-7	1.47	0.9902	0.0922	0.32	0.9948

* The bending response was fitted using a cubic polynomial ($y = \text{Intercept} + B_1 \cdot x + B_2 \cdot x^2 + B_3 \cdot x^3$), while the stretching response was fitted with a linear model (y = Intercept + Slope·x). "y" represents the relative resistance change ($\Delta R/R_0$), and "x" represents the bending angle (°) or tensile strain (%).

Application Demonstration and Degradation Behavior

The practical utility and reliability of Cu/Ag-RCFs were evaluated through cyclic testing and real-world scenario demonstrations. As shown in Fig. 5a and 5b, the sensor exhibited remarkable stability under dynamic mechanical loading. During 20 consecutive bending cycles from 0° to 180°, the resistance response remained highly stable and reversible, fluctuating between approximately 1.5 and 2.6 Ω. This exceptional repeatability, coupled with negligible signal drift, confirms the robustness of the self-assembled scaly conductive structure, which withstands repeated mechanical deformation without delamination or irreversible damage. Similarly, under 20 cycles of 2% tensile strain, the sensor exhibited a durable and reproducible piezoresistive response, with resistance values consistently ranging from 5 to 16 Ω. The consistent and rapid return to baseline resistance after each cycle further validates the elastic behavior of the material in the low-strain regime, underscoring its suitability for monitoring repetitive dynamic motions.

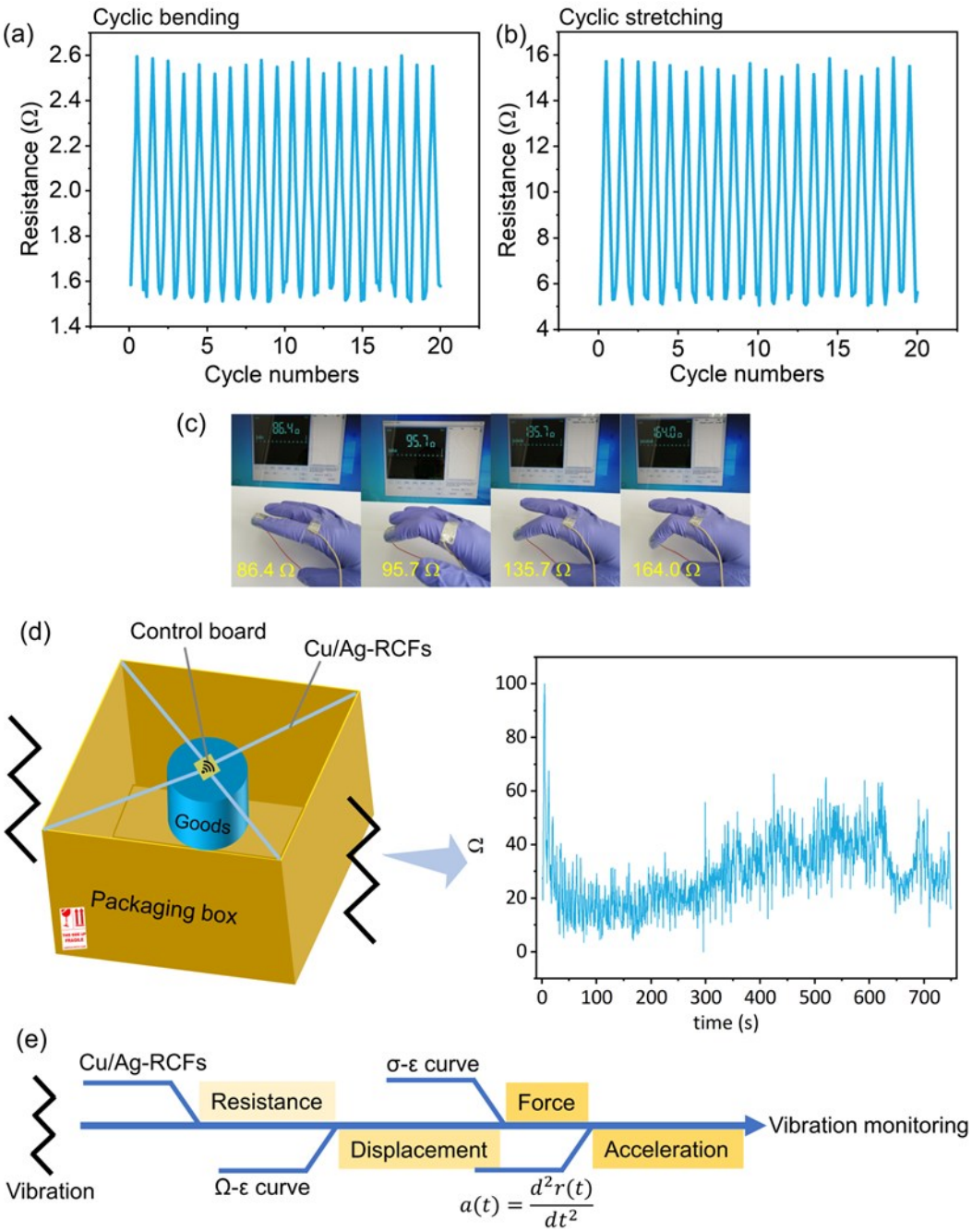

Fig. 5. Demonstration of motion-sensing performance and practical applications of Cu/Ag-RCFs. (a) Real-time resistance response during cyclic bending. (b) Resistance variation under cyclic stretching. (c) Sensor-integrated glove and corresponding real-time resistance changes during finger bending. (d) Schematic of the sensor mounted on a package for vibration monitoring during transportation. (e) Signal conversion workflow: mechanical deformation of Cu/Ag-RCFs is transduced into quantifiable electrical resistance signals.

To demonstrate practical applicability, a sensor was seamlessly integrated into a glove for finger movement monitoring (Fig. 5c). Different bending angles elicited clearly distinguishable and highly reproducible changes in the electrical resistance, varying consistently from 86.4 to 164 Ω. This experiment compellingly illustrates the potential of Cu/Ag-RCFs as a conformable and cost-effective sensing element suitable for next-

generation human-machine interfaces, wearable health monitoring devices, and gesture-controlled systems.

While the current demonstration highlights the feasibility of Cu/Ag-RCFs for real-time gesture recognition, long-term operational stability in uncontrolled environments remains an important consideration. Factors such as mechanical wear, environmental contamination, or gradual oxidation could induce signal drift over extended use, potentially requiring periodic recalibration or integration with machine learning models capable of adaptive pattern recognition (Kong *et al.* 2025). Nevertheless, the high initial reproducibility and robust cyclic performance demonstrated here provide a solid foundation for such future developments.

Beyond biomechanical applications, Cu/Ag-RCFs were also evaluated for their potential in industrial monitoring scenarios. Figure 5d illustrates a proposed deployment for monitoring vibrations and impacts during goods transportation. As depicted in the signal conversion flowchart (Fig. 5e), mechanical vibrations acting on the package induce deformation in the Cu/Ag-RCFs, which is instantaneously converted into quantifiable electrical resistance signals. These signals can be processed to derive key parameters such as acceleration, force, and displacement, providing a comprehensive log of handling conditions during transit. Furthermore, the natural cellulose core of the sensor offers a significant advantage over conventional electronic monitors: end-of-life sustainability. Designed to biodegrade, these sensors can be disposed of with cardboard packaging, thereby mitigating electronic waste associated with permanent monitoring devices.

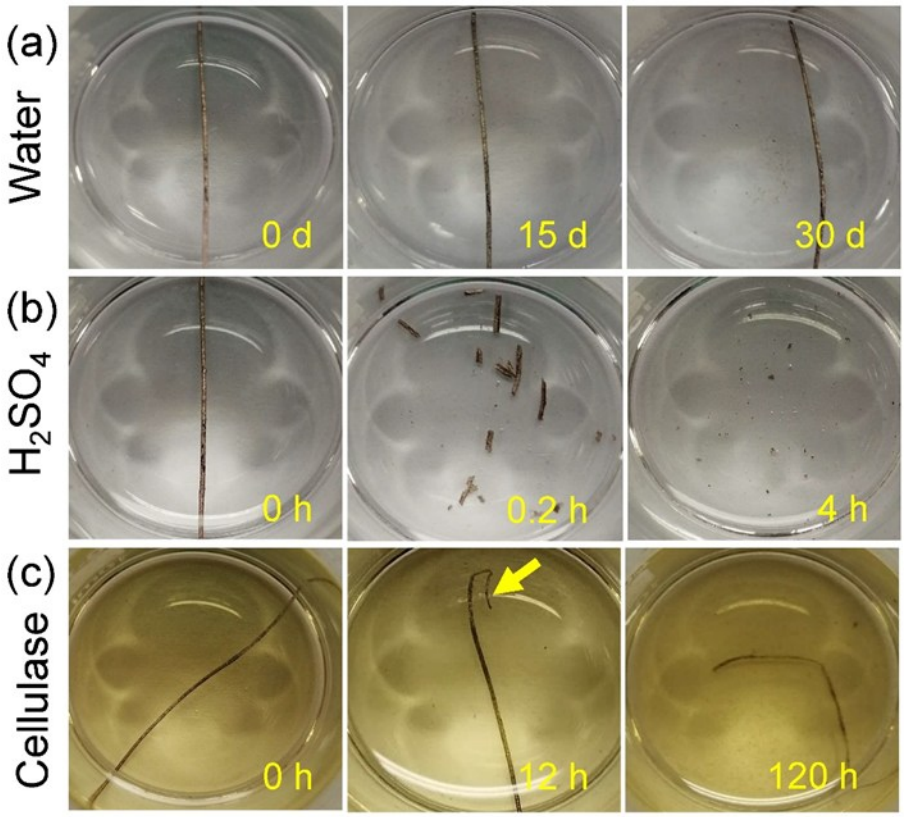

Fig. 6 Degradation behavior of Cu/Ag-RCFs under three representative conditions: (a) immersion in deionized water for 30 days, (b) exposure to 72% sulfuric acid for 4 h, and (c) incubation in a cellulase solution (40 FPU/g) for up to 120 h

The degradation behavior of Cu/Ag-RCFs, a crucial aspect of its environmental sustainability, was systematically investigated (Fig. 6). The sensor maintained structural integrity in deionized water over a 30-day period (Fig. 6a), demonstrating its reliability for short- to medium-term use in common environments. In contrast, exposure to a 72% sulfuric acid solution led to rapid and complete degradation within 4 h (Fig. 6b), highlighting its disintegration capacity under aggressive conditions. More significantly, treatment in a cellulase enzyme solution (40 FPU/g) revealed a biologically driven degradation pathway (Fig. 6c). The cellulose substrate began to break down within 12 h and was fully degraded after 120 h, leaving only the metallic residue. This enzymatic breakdown confirms the biodegradability of the bio-based component and reinforces the eco-friendly design of the sensor, aligning it with circular economy principles.

CONCLUSIONS

1. A facile, scalable, and biomimetic fabrication strategy was developed. A single-step dip-coating process was employed to construct a scaly conductive architecture on regenerated cellulose fibers (RCFs), wherein copper nanoplates and silver nanoparticles self-assemble into a multilayered, overlapping coating during fiber withdrawal. Inspired by the flexible yet protective structure of fish scales, this method is simple, reproducible, cost-efficient, and readily adaptable to large-scale manufacturing.
2. The electromechanical properties of Cu/Ag-RCFs were found to be tunable *via* adjustment of coating cycle number. The number of dip-coating cycles served as an effective and straightforward parameter to tailor sensor performance. Increasing the cycle count enhanced electrical conductivity, mechanical robustness, and sensing range, while preserving excellent flexibility and outstanding cyclic stability. The unique scaly morphology enabled reversible and controllable modulation of inter-flake contact resistance, facilitating sensitive detection across a wide spectrum of deformations—from subtle bending to large tensile strains.
3. High sensing performance with excellent reproducibility and a broad dynamic range was achieved. The optimized sensor (4 coating cycles) exhibited high sensitivity, exceptional signal repeatability ($R^2 > 0.99$), and an extraordinary dynamic response range ($\Delta R/R_0$ spanning several orders of magnitude). Its piezoresistive behavior under tensile strain was highly linear and stable, with an apparent gauge factor ranging from 0.0922 and 0.1070 sufficient for precise and reliable motion monitoring in practical applications.
4. Real-world applicability was successfully demonstrated in diverse scenarios. The Cu/Ag-RCFs were integrated into a glove for real-time finger motion tracking and deployed as a vibration/impact sensor for intelligent logistics. In both cases, the sensors delivered clear, distinguishable, and reproducible electrical responses correlated with mechanical stimuli. These demonstrations highlight their strong potential in next-generation human-machine interfaces, wearable health monitoring systems, intelligent, smart packaging, and industrial condition monitoring.

5. An eco-friendly end-of-life profile supports sustainable electronics. Leveraging a bacterial cellulose-derived substrate, the Cu/Ag-RCFs combine operational reliability with environmental responsibility. The sensor remains structurally stable in ambient aqueous environments yet undergoes rapid and complete biodegradation in acidic or enzymatic conditions. This controlled degradability offers a promising route to mitigate electronic waste and aligns with circular economy principles without sacrificing functional performance during use.

ACKNOWLEDGMENTS

This work was supported by the National Natural Science Foundation of China (22478266) and the Science and Technology Department of Sichuan Province (2022YFH0065).

Conflict of Interest

The authors declare that there is no conflict of interest regarding the publication of this paper.

Use of Generative AI

During the preparation of this work, the authors used DeepSeek-V3 (https://www.deepseek.com/) and Qwen3-Max (https://www.qianwen.com/) for grammar correction and language polishing of the manuscript text. After using this tool, the authors reviewed and edited the content as needed and take full responsibility for the content of the published article. Generative AI was not used to prepare images, figures, graphs, diagrams, to analyze data, to draw scientific conclusions, or to collate references.

REFERENCES CITED

Chen, Z. Y., Yan, T., and Pan, Z. J. (2021). "Review of flexible strain sensors based on cellulose composites for multi-faceted applications," *Cellulose* 28(2), 615-645. https://doi.org/10.1007/s10570-020-03543-6

Gao, W., Ota, H., Kiriya, D., Takei, K., and Javey, A. (2019). "Flexible electronics toward wearable sensing," *Accounts of Chemical Research* 52(3), 523-533. https://doi.org/10.1021/acs.accounts.8b00500

Huang, F., Hu, J. Y., and Yan, X. (2022). "Review of fiber-or yarn-based wearable resistive strain sensors: Structural design, fabrication technologies and applications," *Textiles* 2(1), 81-111. https://doi.org/10.3390/textiles2010005

Huber, T., Graupner, N., and Müssig, J. (2025). "Regenerated cellulose fibres and their composites: From fundamental properties to advanced applications," *Progress in Materials Science*, article 101547.

Kong, X. Z., Wen, W. X., Guan, Y. J., Lin, Z. H., Zheng, J. W., Xie, B. H., Li, S., Xue J. X., and Hu, Q. C. (2025). "Advances in machine learning-driven flexible strain sensors: challenges, innovations, and applications," *ACS Applied Materials & Interfaces* 17(22) 31778-31798. https://doi.org/10.1021/acsami.5c06453

Luo, Y. F., Abidian, M. R., Ahn, J. H., Akinwande, D., Andrews, A. M., Antonietti, M., Bao, Z. N., Berggren, M., Berkey, C. A., Bettinger, C. J., *et al*. (2023). "Technology roadmap for flexible sensors," *ACS Nano* 17(6), 5211-5295. https://doi.org/10.1021/acsnano.2c12606

Ma, S. D., Tang, J., Yan, T., and Pan, Z. J. (2022). "Performance of flexible strain sensors with different transition mechanisms: a review," *IEEE Sensors Journal* 22(8), 7475-7498. https://doi.org/10.1109/JSEN.2022.3156286

Okokpujie, I. P., Tartibu, L. K., Musa-Basheer, H. O., and Adeoye, A. O. M. (2024). "Effect of coatings on mechanical, corrosion and tribological properties of industrial materials: A comprehensive review," *Journal of Bio- and Tribo-Corrosion* 10(2). https://doi.org/10.1007/s40735-023-00805-1

Peng, Y. Y., Yang, N., Xu, Q., Dai, Y., and Wang, Z. Q. (2021). "Recent advances in flexible tactile sensors for intelligent systems," *Sensors* 21(16), article 5392. https://doi.org/10.3390/s21165392

Rajendran, S., Al-Samydai, A., Palani, G., Trilaksana, H., Sathish, T., Giri, J., Saravanan, R., Lalvani, J. I. J., and Nasri, F. (2025). "Replacement of petroleum based products with plant-based materials, green and sustainable energy—A review," *Engineering Reports* 7(4), article e70108. https://doi.org/10.1002/eng2.70108

Saleh, A. K., El-Sayed, M. H., El-Sakhawy, M. A., Alshareef, S. A., Omer, N., Abdelaziz, M. A., Jame, R., Zheng, H. J., Gao, M. G., and Du, H. S. (2025). "Cellulose-based conductive materials for bioelectronics," *ChemSusChem* 18(6), article e202401762. https://doi.org/10.1002/cssc.202401762

Shen, H., Sun, T. Y., and Zhou, J. P. (2023). "Recent progress in regenerated cellulose fibers by wet spinning," *Macromolecular Materials and Engineering* 308(10), article 2300089. https://doi.org/10.1002/mame.202300089

Ummartyotin, S., and Manuspiya, H. (2015). "A critical review on cellulose: From fundamental to an approach on sensor technology," *Renewable and Sustainable Energy Reviews* 41, 402-412. https://doi.org/10.1016/j.rser.2014.08.050

Wang, Q., Nnanna, P. C., Shen, F., Huang, M., Tian, D., Hu, J. G., Zeng, Y. M., Yang, G., and Deng, S. H. (2021). "Full utilization of sweet sorghum for bacterial cellulose production: A concept of material crop," *Industrial Crops and Products* 162, article 113256. https://doi.org/10.1016/j.indcrop.2021.113256

Wang, D. C., Lei, S. N., Zhong, S. J, Xiao, X. D., and Guo, Q. H. (2023). "Cellulose-based conductive materials for energy and sensing applications," *Polymers* 15(20), article 4159. https://doi.org/10.3390/polym15204159

Wang, Q., Zhao, H., Zhao, L., Huang, M., Tian, D., Deng, S. H., Hu, J. G., Zhang, X. Q., and Shen, F. (2023). "Fabrication of regenerated cellulose fibers using phosphoric acid with hydrogen peroxide treated wheat straw in a DMAc/LiCl solvent system," *Cellulose* 30(10), 6187-6201. https://doi.org/10.1007/s10570-023-05263-z

Zhao, D. W., Zhu, Y., Cheng, W. K., Chen, W. S., Wu, Y. Q., and Yu, H. P. (2021). "Cellulose-based flexible functional materials for emerging intelligent electronics," *Advanced Materials* 33(28), article 2000619. https://doi.org/10.1002/adma.202000619

Article submitted: September 10, 2025; Peer review completed: November 1, 2025; Revised version received: February 4, 2026; Accepted: February 5, 2026; Published: April 8, 2026.
DOI: 10.15376/biores.21.2.4607-4619